ORIGINAL ARTICLE

Nanoparticle Delivery of Proangiogenic Transcription Factors into the Neonatal Circulation Inhibits Alveolar Simplification Caused by Hyperoxia

Craig Bolte[1,2], Vladimir Ustiyan[1,2], Xiaomeng Ren[1,2], Andrew W. Dunn[1,2,3], Arun Pradhan[1,2], Guolun Wang[1,2], Olena A. Kolesnichenko[1,2], Zicheng Deng[1,2,3], Yufang Zhang[1,2], Donglu Shi[3], James M. Greenberg[1,4], Alan H. Jobe[1,4], Tanya V. Kalin[1,4], and Vladimir V. Kalinichenko[1,2,4,5]

[1]Department of Pediatrics, University of Cincinnati and Cincinnati Children's Hospital Medical Center, Cincinnati, Ohio; [2]Center for Lung Regenerative Medicine, [4]Division of Pulmonary Biology, and [5]Division of Developmental Biology, Cincinnati Children's Hospital Medical Center, Cincinnati, Ohio; and [3]Materials Science and Engineering Program, College of Engineering and Applied Science, University of Cincinnati, Cincinnati, Ohio

Abstract

Rationale: Advances in neonatal critical care have greatly improved the survival of preterm infants, but the long-term complications of prematurity, including bronchopulmonary dysplasia (BPD), cause mortality and morbidity later in life. Although VEGF (vascular endothelial growth factor) improves lung structure and function in rodent BPD models, severe side effects of VEGF therapy prevent its use in patients with BPD.

Objectives: To test whether nanoparticle delivery of proangiogenic transcription factor FOXM1 (forkhead box M1) or FOXF1 (forkhead box F1), both downstream targets of VEGF, can improve lung structure and function after neonatal hyperoxic injury.

Methods: Newborn mice were exposed to 75% O_2 for the first 7 days of life before being returned to a room air environment. On Postnatal Day 2, polyethylenimine-(5) myristic acid/polyethylene glycol-oleic acid/cholesterol nanoparticles containing nonintegrating expression plasmids with *Foxm1* or *Foxf1* cDNAs were injected intravenously. The effects of the nanoparticles on lung structure and function were evaluated using confocal microscopy, flow cytometry, and the flexiVent small-animal ventilator.

Measurements and Main Results: The nanoparticles efficiently targeted endothelial cells and myofibroblasts in the alveolar region. Nanoparticle delivery of either FOXM1 or FOXF1 did not protect endothelial cells from apoptosis caused by hyperoxia but increased endothelial proliferation and lung angiogenesis after the injury. FOXM1 and FOXF1 improved elastin fiber organization, decreased alveolar simplification, and preserved lung function in mice reaching adulthood.

Conclusions: Nanoparticle delivery of FOXM1 or FOXF1 stimulates lung angiogenesis and alveolarization during recovery from neonatal hyperoxic injury. Delivery of proangiogenic transcription factors has promise as a therapy for BPD in preterm infants.

Keywords: bronchopulmonary dysplasia; neonatal hyperoxic lung injury; nanoparticle gene delivery systems; VEGF signaling; FOX transcription factors

(Received in original form June 24, 2019; accepted in final form April 2, 2020)

Supported by NIH grants HL84151, HL141174, and HL123490 (V.V.K.) and NIH grant HL132849 (T.V.K.).

Author Contributions: C.B. and V.V.K. designed the study. C.B., V.U., X.R., A.W.D., A.P., G.W., O.A.K., Z.D., and Y.Z. conducted experiments. C.B., X.R., A.W.D., D.S., J.M.G., A.H.J., T.V.K., and V.V.K. analyzed the data. C.B., T.V.K., J.M.G., and V.V.K. wrote the manuscript with input from all of the other authors.

Correspondence and requests for reprints should be addressed to Vladimir V. Kalinichenko, M.D., Ph.D., Center for Lung Regenerative Medicine and Division of Pulmonary Biology, Cincinnati Children's Research Foundation, 3333 Burnett Avenue, Cincinnati, OH 45229. E-mail: vladimir.kalinichenko@cchmc.org.

This article has a related editorial.

This article has an online supplement, which is accessible from this issue's table of contents at www.atsjournals.org.

Am J Respir Crit Care Med Vol 202, Iss 1, pp 100–111, Jul 1, 2020

Originally Published in Press as DOI: 10.1164/rccm.201906-1232OC on April 2, 2020
Internet address: www.atsjournals.org

At a Glance Commentary

Scientific Knowledge on the Subject: Advances in neonatal critical care have greatly improved the survival of preterm infants, but the long-term complications of prematurity, including bronchopulmonary dysplasia (BPD), cause mortality and morbidity later in life. Although VEGF (vascular endothelial growth factor) improves lung structure and function in rodent BPD models, severe side effects of VEGF therapy prevent its use in patients with BPD.

What This Study Adds to the Field: Using nanoparticle delivery of VEGF target genes *FOXM1* (forkhead box M1) and *FOXF1* (forkhead box F1) directly into the pulmonary microvasculature, we found that FOXM1 and FOXF1 nonintegrating expression vectors increased endothelial proliferation and lung angiogenesis after neonatal hyperoxic injury in a mouse model of BPD. FOXM1 and FOXF1 improved elastin fiber organization, decreased alveolar simplification, and preserved lung function in mice reaching adulthood. Our results suggest that nanoparticle delivery of proangiogenic transcription factors can be a promising therapeutic option to treat BPD associated with pulmonary vascular disease.

Recent advances in nanotechnology have demonstrated that nanoparticles can be used for therapeutic purposes. To date, nanoparticles have been constructed using a number of materials and have been shown to be effective over a range of sizes for selective delivery to specific tissues. Nanoparticles can deliver organic and nonorganic compounds and molecules into cells, including coding DNAs and mRNAs for gene expression. Nanoparticle delivery systems have been used clinically and experimentally to treat cancer, inflammatory conditions, and complications of diabetes and have demonstrated potential for use in tissue regeneration. Nanoparticle-based therapies can inhibit growth of non–small cell lung cancer (1), improve alveolar structure in chronic obstructive pulmonary disease (2), stimulate wound healing in patients with diabetes (3), and increase microvascular density when applied topically *ex vivo* to airway transplants (4). These studies highlight the therapeutic potential of nanoparticle technology, and further advances in this field will improve tissue specificity and efficiency of these applications.

Bronchopulmonary dysplasia (BPD) is a well-described complication of preterm birth, especially in those born before 28 weeks of gestation. Affected infants experience chronic respiratory insufficiency requiring support with supplemental oxygen and, in severe cases, long-term positive pressure ventilation (5). Since its initial description in 1967 (6), the pathophysiologic characteristics of BPD have evolved in parallel with improvements in clinical care, including exogenous surfactant replacement and sophisticated mechanical ventilation strategies. Today, there is general agreement that for a given patient, BPD involves varying components of parenchymal, vascular, and conducting airway disease (7, 8). Of these, there is growing recognition that the vascular component of BPD exerts a major impact on disease progression and severity. After premature birth, transition of the lung to a nonaqueous environment appears sufficient to disrupt subsequent alveolar growth and the attendant vascular structures required for effective gas exchange (8, 9). This is further exacerbated when the preterm lung is exposed to supplemental oxygen and positive pressure ventilation. Interestingly, inhibition of vascular growth in preterm rodent models impairs alveolar development (5, 8). Diminished expression of VEGF-A (vascular endothelial growth factor A) and PECAM-1 (platelet endothelial cell adhesion molecule 1) in the lungs of infants with severe BPD (9) provides additional evidence that pulmonary vascular growth is a central driver of lung development and suggests that therapeutic interventions to support pulmonary vascular growth might promote growth of alveolar structures. Consistent with this hypothesis, administration of VEGF in rodent models of BPD improved lung angiogenesis and alveolarization (5, 10, 11). However, VEGF administration in animal models also caused pulmonary edema and hemorrhage. Therefore, alternative strategies for improving postnatal lung angiogenesis deserve investigation.

The FOX (forkhead box) proteins comprise a large family of winged helix transcription factors shown to be downstream mediators of several developmental signaling pathways, including the VEGF pathway (12–17). Deletion of either the *Foxm1* (forkhead box M1) or *Foxf1* (forkhead box F1) gene in mice reduces proliferation of pulmonary endothelial cells during lung development and lung repair after injury (18–21). FOXM1 and FOXF1 induce expression of VEGF receptor 2 (Flk1 or KDR), stimulating VEGF/Flk1 signaling *in vitro* and *in vivo* (20, 22). Mutations in the *FOXF1* gene are associated with alveolar capillary dysplasia with misalignment of pulmonary veins (23, 24), a severe congenital disorder associated with the primary loss of alveolar capillaries and respiratory insufficiency shortly after birth (25). FOXF1 stimulates proliferation of endothelial cells and accelerates lung regeneration after partial pneumonectomy (19). Given proangiogenic functions of FOXF1 and FOXM1 in the VEGF/Flk1 signaling pathway, it is unclear whether these transcription factors can be delivered to neonatal pulmonary vasculature and stimulate angiogenesis *in vivo*. In this study, we evaluated the ability of newly developed polyethylenimine-(5) myristic acid/polyethylene glycol oleic acid/cholesterol (PEI_{600}-MA_5/PEG-OA/Cho) nanoparticles (26) to deliver proangiogenic cDNA expression vectors into the pulmonary circulation with the purpose of improving angiogenesis and alveolarization after neonatal hyperoxic injury.

Methods

Ethics Statement

The data, analytic methods, and study materials will be made available to other researchers from the corresponding author of this article upon request for purposes of reproducing the results or replicating the procedures. All procedures were performed in accordance with Association for Assessment and Accreditation of Laboratory Animal Care International guidelines and were approved by the Cincinnati Children's Research Foundation Institutional Animal Care and Use

Committee. NIH guidelines for laboratory animal care and safety were strictly followed.

Mice and Neonatal Hyperoxia

Wild-type C57BL/6 mice were used for all studies. BPD-like phenotype was induced by exposing newborn mice to 75% O_2 for 7 days (Postnatal Days [P] P1–P7), with both male and female neonatal mice used for analysis (27). On P2, mice were briefly removed from the hyperoxic chamber, and nanoparticles containing either an empty cytomegalovirus (CMV) vector or CMV expression plasmid containing either *Foxf1* or *Foxm1* cDNA were injected via the facial vein. Mice were then immediately returned to the hyperoxic chamber. On P7, mice were placed in a room air environment.

Nanoparticles

PEI_{600}-MA_5/PEG-OA/Cho nanoparticles were synthesized and labeled with DyLight 650 quantum dots (Thermo Fisher Scientific) as described elsewhere (24, 26). *CMV-Foxf1*, *CMV-Foxm1*, *CMV-GFP* (CMV-green fluorescent protein), or *CMV-empty* nonintegrating expression plasmids (28–31) were incapsulated into the nanoparticles at a mass ratio of 24:1 (polymer/DNA). Without plasmid DNA, nanoparticles were significantly larger, limiting their use *in vivo*. *CMV-Foxf1* contained *CMV* promoter and HA (hemagglutinin)-tagged mouse *Foxf1* cDNA cloned into the pShuttle expression vector (Addgene). *CMV-Foxm1* contained *CMV* promoter and Flag-tagged mouse *Foxm1* cDNA cloned into the pMIEG3 expression vector. P2 pups were administered an injection with 5 μg of plasmid DNA (120-μg nanoparticles) in a single 25-μl bolus intravenously via the facial vein.

Histology and Immunostaining

Lung sections were stained with hematoxylin and eosin or used in immunostaining as previously described (32–35) with the following antibodies (Abs): PECAM-1 (1:100; Abcam), endomucin (1:100; Abcam), Ki-67 (1:200; BD Pharmingen), MAC3 (1:50; BD Pharmingen), ERG (ETS transcription factor ERG) (1:250; Abcam), and αSMA (α-smooth muscle actin) (1:5,000; MilliporeSigma). Elastin staining was performed using Weigert's elastic stain (Poly Scientific R&D Corp.) according the manufacturer's instructions. Changes in alveolar structure were determined as previously described (27). Complexity of the endothelial network in the lung was evaluated using confocal imaging of endomucin-stained lung sections and labeling of perfused blood vessels with isolectin B4 as described previously (24, 36).

qRT-PCR and Western Blotting

Total RNA isolation, reverse transcription, and qRT-PCR analysis were performed

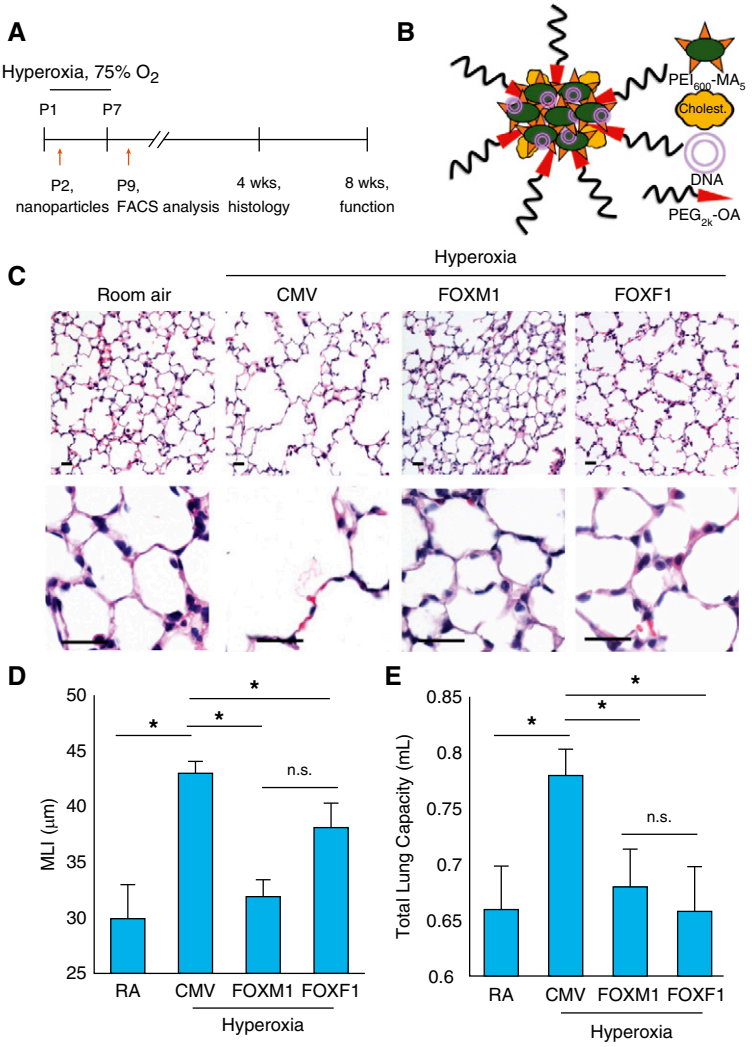

Figure 1. Nanoparticle delivery of FOXM1 (forkhead box M1) or FOXF1 (forkhead box F1) decreases alveolar simplification caused by neonatal hyperoxia. (*A*) Schematic representation of 7-day hyperoxia treatment of wild-type newborn mice. Control mice were exposed to room air (RA). Polyethylenimine-(5) myristic acid/polyethylene glycol oleic acid/cholesterol (PEI_{600}-MA_5/PEG-OA/Cho) nanoparticles were delivered at Postnatal Day 2 (P2) via the facial vein. (*B*) Structure of PEI_{600}-MA_5/PEG-OA/Cho nanoparticles containing plasmid DNA, PEI_{600}-MA_5, and polyethylene glycol oleic acid (PEG_{2k}-OA). (*C*) Hematoxylin and eosin (H&E) staining of paraffin-embedded lung sections shows alveolar simplification in hyperoxia-treated mice. Mice were exposed to hyperoxia or RA from P1 to P7, followed by RA exposure until lung harvest at P28. Nanoparticle delivery was performed at P2. Delivery of either FOXM1 or FOXF1 expression vectors improves lung structure in hyperoxia-treated mice compared with cytomegalovirus (CMV)-empty control. Scale bars, 50 μm. (*D*) Nanoparticle delivery of FOXM1 or FOXF1 decreases alveolar simplification. Mean linear intercept (MLI) was calculated using 15 random H&E–stained lung fields ($n = 4$–6 mice per group). (*E*) Nanoparticle delivery of FOXM1 or FOXF1 normalizes TLC in hyperoxia-treated mice. TLC was measured using the flexiVent ventilator when mice were 8 weeks of age ($n = 4$–6 mice per group). Error bars are mean ± SE. *$P < 0.05$. FACS = fluorescence-activated cell sorter; n.s. = not significant.

as previously described (37–40) using inventoried Applied Biosystems TaqMan mouse *Foxo1*(forkhead box O1), *Flk1*, and *Vegfa* probes (Thermo Fisher Scientific). Western blot analysis was performed on protein lysate isolated from whole lung as previously described (41, 42).

Flow Cytometry

Flow cytometry was performed on single-cell suspensions generated from enzyme-digested lung tissue as previously described (43, 44). Live cells were identified with 7-aminoactinomycin D (7-AAD). Hematopoietic cells were identified by CD45 Abs (clone 30-F11; eBioscience). The $CD45^-$ population was then evaluated for the presence of CD31 (clone 390; eBioscience) and CD326 (clone G8.8; eBioscience) for identification of endothelial ($CD31^+CD45^-CD326^-$) and epithelial cells ($CD326^+CD45^-CD31^-$). Cells not expressing any of these markers ($CD45^-CD31^-CD326^-$) were then evaluated for pericytes ($PDGFRb^+NG2^+CD45^-CD31^-CD326^-$) using PDGFRb (platelet-derived growth factor receptor-β) (CD140b) Ab (clone APB5; BioLegend) and NG2 (melanoma-associated chondroitin sulfate proteoglycan 4) Ab (clone 9.2.27; BD Biosciences). PDGFRa (platelet-derived growth factor receptor-α) (CD140a) Ab (clone APA5; BD Biosciences) were used to identify myofibroblasts ($PDGFRa^+CD45^-CD31^-CD326^-$). Cell cycle analysis was performed by measuring DNA content using Hoechst 33342 (Thermo Fisher Scientific). Stained cells were analyzed using a five-laser FACSAria II cell sorter (BD Biosciences). Plasmid-derived *Foxf1* mRNA was detected in fluorescence-activated cell sorter (FACS)-sorted endothelial cells and myofibroblasts using RT-PCR with the following primers: forward *HA* primer, 5′-TACCCATACG ATGTTCCAGATTACGCT-3′; reverse *Foxf1* primer, 5′-AGTGGCTGGGCAAA GCCATG-3′. RT-PCR data were generated using 10–30 cycles.

Measurement of Lung Function

Lung function was evaluated using the flexiVent small-animal ventilator (SCIREQ) as previously described (27, 45). A total of four to six mice were evaluated per group at 8 weeks of age.

Statistical Analysis

One-way ANOVA and Student's *t* test were used to determine statistical significance. The logarithmic transformation was applied for skewed data to confirm normality. *P* values less than or equal to 0.05 were considered statistically significant. All data were presented as mean ± SE or mean ± SD.

Results

Nanoparticle Delivery of FOXM1 or FOXF1 Prevents Alveolar Simplification Caused by Hyperoxic Injury

Mice were subjected to hyperoxia (75% O_2) for the first week of life and then returned to room air at P7 (Figure 1A). Lung histology was analyzed at 4 weeks of age. Delivery of *CMV-Foxm1* and *CMV-Foxf1* plasmids (abbreviated as "FOXM1" and "FOXF1," respectively) was performed intravenously at P2 using PEI_{600}-MA_5/PEG-OA/Cho nanoparticles (Figure 1B) capable of delivering nonintegrating DNA expression plasmids into pulmonary endothelium with high efficiency (26). The hydrodynamic diameter and surface charge of PEI_{600}-MA_5/PEG-OA/Cho nanoparticles mixed with plasmid DNA were 153 ± 68 nm and +18.3 ± 5.2 mV, respectively (Figures E1A–ED in the online supplement).

Consistent with published studies (5, 10, 11, 27), neonatal hyperoxia exposure caused alveolar simplification, as shown by hematoxylin and eosin staining of P28 lungs (Figures 1C and 1D). Administration of nanoparticles containing either FOXM1 or FOXF1 improved lung morphology (Figure 1C) and decreased alveolar size (Figure 1D). There was no difference in lung histology between mice exposed to hyperoxia alone and mice exposed to hyperoxia in combination with nanoparticle delivery of control *CMV-empty* plasmid (Figure E2). Consistent with alveolar simplification, neonatal hyperoxic

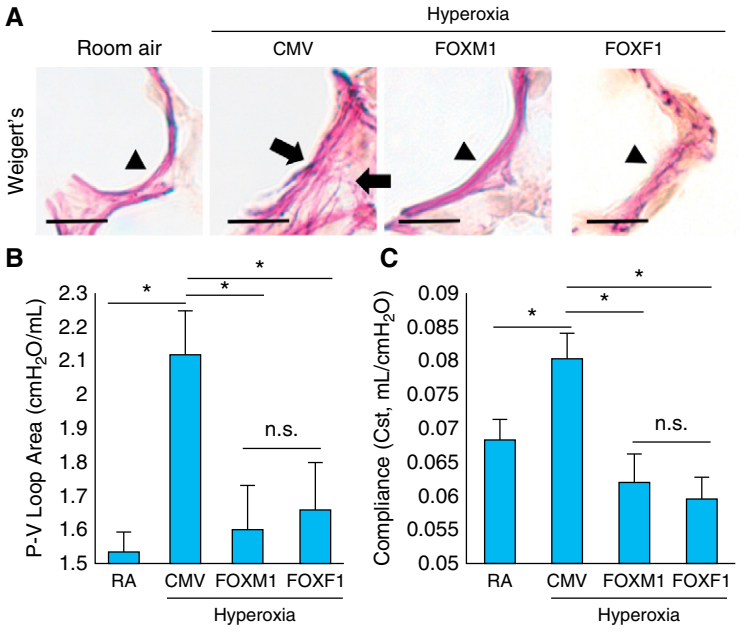

Figure 2. Nanoparticle delivery of FOXM1 (forkhead box M1) or FOXF1 (forkhead box F1) improves lung function in hyperoxia-treated lungs. (*A*) Elastin staining of paraffin-embedded lung sections shows disorganization of elastin fibers in hyperoxia-treated lungs (arrows). Mice were exposed to hyperoxia or room air (RA) from Postnatal Day 1 (P1) to P7, followed by RA exposure until lung harvest at P28. Nanoparticle delivery was performed at P2. Delivery of either FOXM1 or FOXF1 expression vectors improves elastin fiber deposition in alveolar septa of hyperoxia-treated mice. Arrowheads show normal elastic fibers. Scale bars, 50 μm. (*B* and *C*) Nanoparticle delivery of FOXM1 or FOXF1 improves lung function in hyperoxia-treated mice. Pressure–volume (P-V) loop area and lung compliance were measured using the flexiVent ventilator when mice were 8 weeks of age (n = 4–6 mice per group). Error bars are mean ± SE. *$P < 0.05$. CMV = cytomegalovirus; n.s. = not significant.

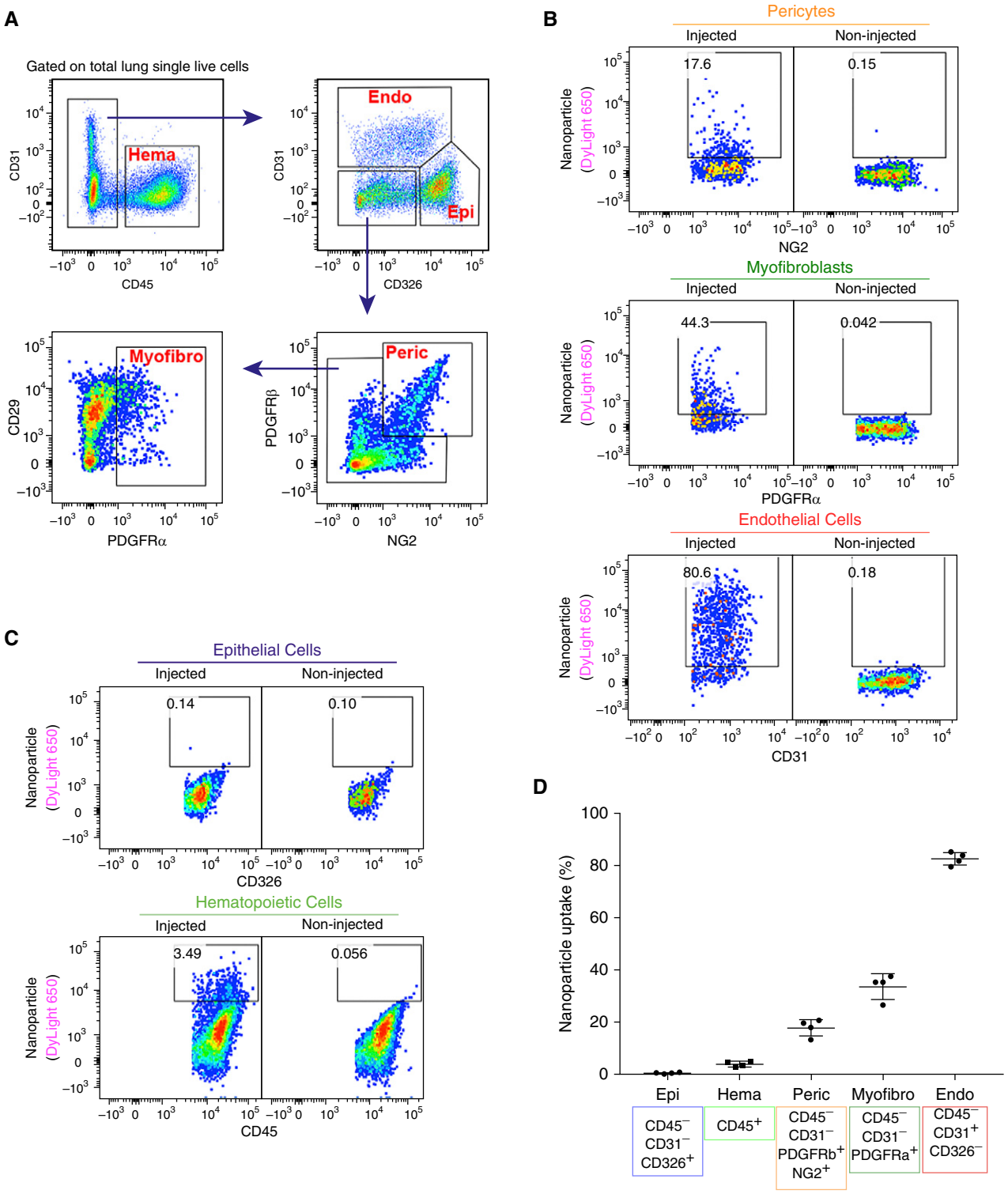

Figure 3. Polyethylenimine-(5) myristic acid/polyethylene glycol oleic acid/cholesterol (PEI_{600}-MA_5/PEG-OA/Cho) nanoparticles efficiently target endothelial cells in the neonatal lung. (*A*) Fluorescence-activated cell sorter (FACS) gating strategy to identify hematopoietic cells (Hema; $CD45^+CD31^-$), endothelial cells (Endo; $CD31^+CD45^-CD326^-$), epithelial cells (Epi; $CD326^+CD45^-CD31^-$), pericytes (Peric; $NG2^+PDGFRb^+CD45^-CD31^-CD326^-$), and myofibroblasts (Myofibro; $PDGFRa^+CD45^-CD31^-CD326^-$). DyLight 650–labeled nanoparticles were delivered at Postnatal Day 2 (P2). FACS analysis of enzymatically digested lung tissue was performed at P5. (*B* and *C*) Dot plots show the presence of nanoparticles in different populations of pulmonary cells. Noninjected mice were used as control animals to identify cells containing nanoparticles. (*D*) Percentage of nanoparticle-targeted cells is shown among pericytes; myofibroblasts; and epithelial, endothelial, and hematopoietic cells ($n = 4$ mice per group). Error bars are mean ± SE. NG2 = melanoma-associated chondroitin sulfate proteoglycan 4; PDGFRα = platelet-derived growth factor receptor-α; PDGFRβ = platelet-derived growth factor receptor-β.

injury increased TLC at 8 weeks of age (Figure 1E). Nanoparticle delivery of FOXM1 or FOXF1 reduced TLC to levels seen in mice exposed to room air (Figure 1E). Furthermore, alveolar elastin fibers were disorganized in hyperoxia-treated lungs, but this was improved by nanoparticle delivery of FOXM1 or FOXF1 (Figure 2A). Consistent with improvement of lung structure, lung function parameters such as pressure–volume loop area and compliance returned to normal values (Figures 2B and 2C). Thus, nanoparticle delivery of FOXM1 or FOXF1 into the neonatal circulation decreases alveolar simplification and improves lung function after hyperoxic injury.

PEI_{600}-MA_5/PEG-OA/Cho Nanoparticles Effectively Target Endothelial Cells in the Neonatal Lung

To identify pulmonary cell types targeted by the PEI_{600}-MA_5/PEG-OA/Cho nanoparticles in the neonatal lung, the polymer–DNA complexes were labeled with DyLight 650 quantum dots and injected into the circulation of P2 mice. Three days later, FACS analysis for cell surface markers was performed using single-cell suspensions derived from enzymatically digested lung tissue (Figure 3A). DyLight 650 fluorescence was detected in 80% of pulmonary endothelial cells ($CD31^+CD45^-CD326^-$), 20% of pericytes ($NG2^+PDGFRb^+CD45^-CD31^-$), and 35% of myofibroblasts ($PDGFRa^+CD45^-CD31^-$) (Figures 3B and 3D). In contrast, no nanoparticle uptake was observed in hematopoietic cells ($CD45^+$) and epithelial cells ($CD326^+CD45^-CD31^-$) (Figures 3C and 3D). The presence of nanoparticles in endothelial cells was detected by FACS analysis for GFP, which was performed 3 days after injection of *CMV-GFP* reporter plasmid encapsulated into the nanoparticles (Figures 4A and 4B). GFP was detected in cells expressing endothelial markers endomucin and CD31 (PECAM-1) (Figures 4C, 4D, E3A, and E3B). GFP was present in perinuclear regions of endothelial cells that are abundant with ribosomes (Figures 4C and 4D), consistent with active translation of GFP protein. GFP reporter was active in endothelial cells at P5 and P7 (Figure 4B). GFP was undetectable in hematopoietic and epithelial cells (Figures 4A and 4B). Furthermore, we used RT-PCR to detect

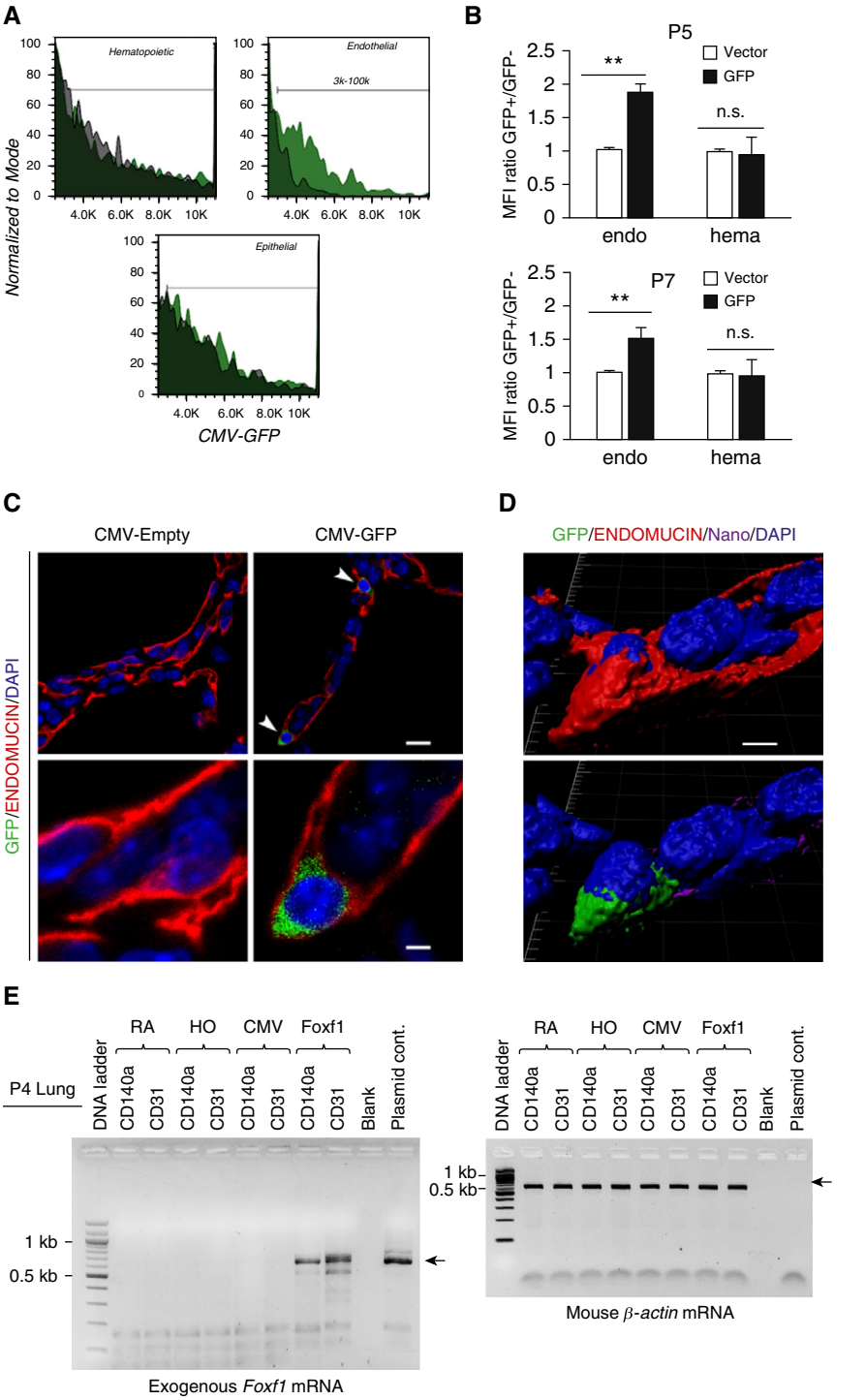

Figure 4. Polyethylenimine-(5) myristic acid/polyethylene glycol oleic acid/cholesterol (PEI_{600}-MA_5/PEG-OA/Cho) nanoparticles deliver cytomegalovirus (CMV)-GFP (green fluorescent protein) reporter plasmid to pulmonary endothelial cells. (*A* and *B*) GFP fluorescence is detected in pulmonary endothelial cells after treatment with PEI_{600}-MA_5/PEG-OA/Cho nanoparticles. CMV-GFP plasmid was encapsulated into nanoparticles, and the nanoparticle–DNA complexes were injected at Postnatal Day 2 (P2). Lungs were harvested at P5 and P7 and used for fluorescence-activated cell sorter (FACS) analysis. Histograms in *A* show GFP fluorescence in different cell types. GFP (green area) is detected in endothelial cells ($CD31^+CD45^-CD326^-$). Autofluorescence is shown as the black area. Data were quantitated in *B* by comparing GFP mean fluorescence intensity (MFI) with

exogenous, plasmid-derived *Foxf1* mRNA in FACS-sorted endothelial cells and myofibroblasts. Consistent with DyLight 650 labeling of the nanoparticles (Figure 3B), exogenous *Foxf1* mRNA was detected in both endothelial cells and myofibroblasts at P4 (Figure 4E). The expression level of exogenous *Foxf1* mRNA was higher in endothelial cells than in myofibroblasts (Figure E4A). At P12, exogenous *Foxf1* mRNA was undetectable in FACS-sorted cells (Figures E4B and E4C).

Interestingly, GFP was observed in pulmonary microvascular endothelial cells but not in endothelial cells of large blood vessels (Figure E5), a finding consistent with our recent studies (26). When delivered intratracheally, the PEI_{600}-MA_5/PEG-OA/Cho nanoparticles did not target endothelial cells or any other cell types in the lung (Figure E6). Thus, PEI_{600}-MA_5/PEG-OA/Cho nanoparticles efficiently deliver DNA expression plasmids into microvascular endothelial cells and myofibroblasts after intravenous administration.

Nanoparticle Delivery of FOXM1 or FOXF1 Increases Lung Angiogenesis after Hyperoxic Injury

Consistent with published studies (8, 9), neonatal hyperoxia exposure decreased capillary density in the lung, as shown by immunostaining and confocal imaging for the endothelial marker endomucin (Figures 5A, 5C, and E7A). Nanoparticle delivery of FOXM1 or FOXF1 increased capillary density in alveolar regions, as shown by endomucin staining (Figures 5A, 5C, and E7A) and by intravascular labeling with isolectin B4 (Figures 5B, 5D, and E7B). Increased endothelial coverage in alveoli was confirmed by PECAM-1 immunostaining (Figure E8). Increasing the dose of *CMV-Foxm1*–nanoparticle complexes did not further improve capillary density and alveolar size (Figures E9A–E9D). Delivery of either *CMV-Foxm1* or *CMV-Foxf1* plasmids without nanoparticles was ineffective (Figures E10A–E10D).

Interestingly, administration of nanoparticles containing either FOXM1 or FOXF1 decreased hyperoxia-associated remodeling of pulmonary arteries and prevented smooth muscle thickening of arterial walls (Figures E11A–E11E). Nanoparticle treatments of room air–exposed mice had no effect on neonatal angiogenesis and alveolarization (Figures E12A–E12D). Altogether, nanoparticle delivery of either FOXM1 or FOXF1 into the neonatal circulation increases capillary density and decreases arterial remodeling after hyperoxic injury.

Nanoparticle Delivery of FOXM1 or FOXF1 Does Not Protect Endothelial Cells from Cell Death Caused by Hyperoxia

When mice were examined at the end of hyperoxia exposure at P7, loss of body weight occurred in all hyperoxia-treated groups independently of nanoparticle treatment (Figure E13A). Alveolar simplification was evident in all hyperoxia-treated groups at P7 (Figure E13B). Consistent with published studies (8, 9), hyperoxia exposure decreased the total number of pulmonary endothelial cells (determined by FACS), and this was unaltered by the choice of polymer–DNA complexes (Figure E13C). Furthermore, endothelial cells were equally targeted by the nanoparticles, regardless of plasmid DNA used for packaging (Figure E13D). Next, we examined if delivery of FOXM1 or FOXF1 protects endothelial cells from cell death caused by hyperoxia. FACS analysis using 7-AAD viability dye showed that nanoparticle delivery of FOXM1 or FOXF1 did not change percentages of 7-AAD^+ endothelial cells in the lung tissue compared with *CMV-empty* control (Figures E14A and E14B). There was no difference in cell death between endothelial cells containing the nanoparticles and endothelial cells without nanoparticles (Figures E14C). Interestingly, all nanoparticle treatments increased mRNAs of *Flk1* and *Vegfa* in hyperoxia-treated lungs at P7 (Figure E15). However, in contrast to *CMV-Foxm1* and *CMV-Foxf1*, *CMV-empty* was unable to increase capillary density at P14 and P28 (Figure 5). Altogether, neither FOXM1 nor FOXF1 protects endothelial cells from cell death caused by neonatal hyperoxic injury.

Nanoparticle Delivery of FOXM1 or FOXF1 Enhances Endothelial Cell Proliferation during Recovery from Hyperoxic Injury

Western blot and qRT-PCR analyses of lung tissue demonstrated that nanoparticle delivery of either FOXM1 or FOXF1 decreased protein and mRNA of *Foxo1* (Figures 6A and 6B), a transcription factor that inhibits the progression of endothelial cells into the cell cycle (46). In contrast, protein amounts of proproliferative CCND1 (cyclin D1) and FLK1, both downstream targets of the VEGF signaling pathway (5, 47), were increased by FOXM1 or FOXF1 nanoparticle delivery (Figures 6C and 6D). Given the altered expression of cell cycle regulatory genes and increased vascularity after nanoparticle delivery of FOXM1 or FOXF1, we tested if endothelial cell proliferation is the mechanism by which the nanoparticle–DNA complexes increase angiogenesis after hyperoxic injury. Cell cycle analysis for DNA dye Hoechst 33342 was performed by FACS in pulmonary endothelial cells at P9, 2 days after hyperoxic exposure was completed and mice were returned to a room air environment (Figures 7A and 7B). Compared with *CMV-empty* control, nanoparticle delivery of FOXM1 or FOXF1 increased the percentage of

Figure 4. (*Continued*). autofluorescence in each cell type ($n = 3$–4 mice per group). Error bars are mean ± SE. $^{**}P < 0.01$. (*C*) Confocal images show that GFP is present in perinuclear regions of endothelial cells stained with endomucin (arrowheads). Lungs of mice treated with nanoparticles containing CMV–empty plasmid were used as controls. Scale bars: top panels, 10 μm; bottom panels, 2 μm. (*D*) High-magnification confocal images show the presence of GFP (green) and DyLight 650 quantum dots (purple) in cytoplasm of microvascular endothelial cells stained with endomucin. Cell nuclei were stained with DAPI (blue). Cell surface endomucin was removed using a deconvolution option in Imaris software (imaris.oxinst.com) (bottom image), indicating the presence of GFP and DyLight 650 inside the cell. Scale bars, 2 μm. (*E*) RT-PCR shows the presence of exogenous, plasmid-derived Foxf1 (forkhead box F1) mRNA in endothelial cells ($CD31^+CD45^-CD326^-$) and myofibroblasts ($CD140a^+CD31^-CD45^-CD326^-$) that were FACS sorted from P4 lungs. β-Actin was used as a loading control. endo = endothelial cells; hema = hematopoietic cells; HO = hyperoxia; n.s. = not significant; RA = room air.

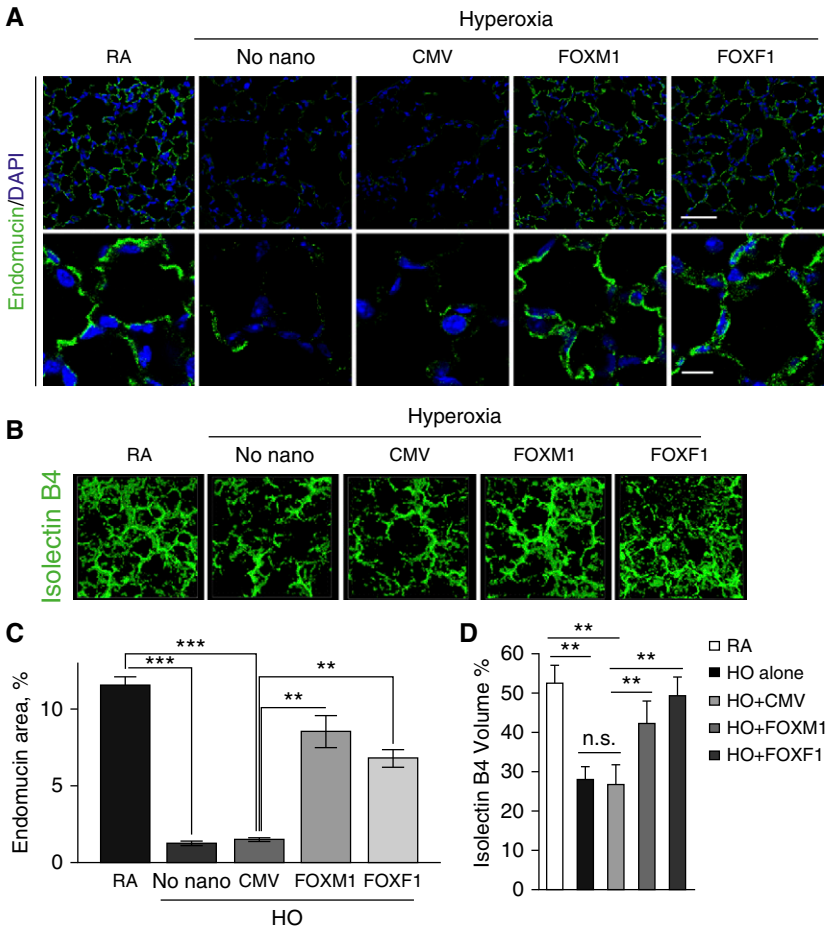

Figure 5. Nanoparticle delivery of FOXM1 (forkhead box M1) or FOXF1 (forkhead box F1) improves alveolar microvascular network in hyperoxia (HO)-treated mice. (*A*) Immunostaining for endomucin shows alveolar microvascular networks (green) in P28 lungs. Mice were exposed to HO or room air (RA) from Postnatal Day 1 (P1) to P7, followed by RA exposure until lung harvest at P28. Nanoparticles containing cytomegalovirus (CMV)-Foxm1, CMV-Foxf1, or CMV-empty (control) were delivered at P2. DAPI was used to stain cell nuclei. The alveolar microvascular network is improved after nanoparticle delivery of FOXM1 or FOXF1. Scale bars: top panels, 50 μm; bottom panels, 10 μm. (*B*) Nanoparticle delivery of FOXM1 or FOXF1 increases capillary density in HO-injured lungs. Isolectin B4 was injected i.v. 1 hour before harvesting the mice at P14 ($n = 3$–4 mice per each group). (*C* and *D*) Endomucin-stained area (*C*) and isolectin B4–labeled volume (*D*) were quantified using 10 random lung images ($n = 3$–6 mice per group). Error bars are mean ± SD. $^{**}P < 0.01$ and $^{***}P < 0.001$. n.s. = not significant.

endothelial cells undergoing S, G_2, and M phases of the cell cycle (Figures 7B and 7C). The number of Ki-67$^+$ endothelial cells was increased after nanoparticle delivery of FOXM1 or FOXF1 (Figures E16A and E16C). In contrast, proliferation of hematopoietic (CD45$^+$) and epithelial cells (CD326$^+$CD45$^-$CD31$^-$) was unaltered, as shown by FACS analysis (Figure 7C). The number of Ki-67$^+$ macrophages was unchanged after the nanoparticle treatment (Figures E16B and E16D). Interestingly, nanoparticles were still present in endothelial cells at P9, and when endothelial cells were compared on the basis of presence or absence of nanoparticles, it was evident that proliferation was only enhanced in the population of endothelial cells that had uptaken the nanoparticles (Figure 7D). Altogether, nanoparticle delivery of FOXM1 and FOXF1 accelerates endothelial cell proliferation during recovery after neonatal hyperoxic injury, leading to increased angiogenesis and alveolarization.

Discussion

BPD is a serious complication of prematurity with limited treatment options for the prevention of long-term pulmonary developmental sequelae. Advanced respiratory support and antenatal glucocorticoid treatment in preterm infants have resulted in a dramatic increase in infant survival; however, these therapies do not reduce the incidence of BPD. Decreased pulmonary vascular development is a pathophysiologic hallmark of BPD that has been demonstrated in both human patients and animal models (8, 9, 48). Therefore, stimulation of neonatal lung angiogenesis is a promising strategy to improve postnatal lung development in preterm infants. In this study, we used the PEI_{600}-MA_5/PEG-OA/Cho formulation of nanoparticles to deliver nonintegrating expression vectors into the neonatal circulation with the purpose of improving lung structure and function in hyperoxia-treated mice. We found that nanoparticle-mediated expression of the proangiogenic transcription factors FOXM1 and FOXF1 in the early postnatal period is sufficient to improve postnatal lung development and, ultimately, lung function in mice injured by hyperoxia. Interestingly, nanoparticle treatment did not protect pulmonary endothelial cells from cell death caused by hyperoxic injury, as evidenced by lack of changes in endothelial cell viability at the end of hyperoxia treatment. However, the nanoparticle treatment increased endothelial proliferation and lung angiogenesis after the injury.

Both FOXM1 and FOXF1 promoted endothelial proliferation downstream of VEGF, which acts through VEGF receptor 2 (Flk1 or KDR) to stimulate angiogenesis (20, 22). Published studies supported the efficacy of VEGF therapy for protection from hyperoxic injury in rodent models of alveolar simplification. However, pulmonary edema, a side effect of systemic VEGF administration (5, 49), was not observed in the present study. This indicates a significant advantage of nanoparticle delivery of VEGF-regulated FOXM1 and FOXF1 directly into endothelial cells because edema could have

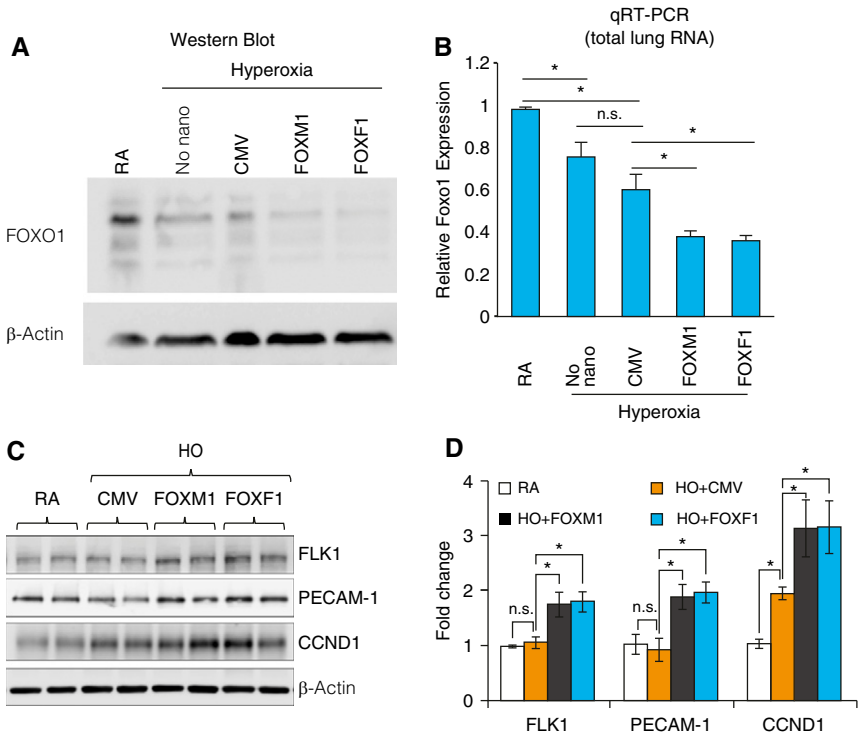

Figure 6. Nanoparticle delivery of FOXM1 (forkhead box M1) or FOXF1 (forkhead box F1) alters expression of cell cycle regulatory genes in hyperoxia (HO)-treated lungs. (*A*) Immunoblots show the amounts of FOXO1 (forkhead box O1) and β-actin proteins in lung extracts after nanoparticle delivery of FOXM1 or FOXF1. Mice were exposed to HO or room air (RA) from Postnatal Day 1 (P1) to P7, followed by RA exposure. Nanoparticle–DNA complexes were injected at P2. Cytomegalovirus (CMV)–empty plasmid was used as a control. (*B*) qRT-PCR shows the expression of Foxo1 mRNA in whole-lung RNA after nanoparticle delivery of FOXM1 or FOXF1 ($n = 3$ mice per group). Foxo1 mRNA was normalized to β-actin mRNA. (*C* and *D*) Immunoblots show expression of FLK1 (vascular endothelial growth factor receptor 2), PECAM-1 (platelet endothelial cell adhesion molecule 1), and CCND1 (cyclin D1) in lung protein extracts after nanoparticle delivery of FOXM1 or FOXF1. Images were quantified using densitometry ($n = 3$–4 mice per group). Error bars are mean ± SE. $^*P < 0.05$. n.s. = not significant.

deleterious effects on lung development in addition to exacerbating the compromised lung function in infants with BPD. Interestingly, we observed beneficial effects of nanoparticle–*CMV-empty* complexes on expression of proangiogenic mRNAs, raising the possibility that nanoparticles by themselves or in complex with nucleotides can influence gene expression. Although we cannot rule out potential off-target effects of the nanoparticles, the *CMV-empty*–induced changes in gene expression did not result in long-term improvements in angiogenesis and alveolarization, as were observed after nanoparticle delivery of *CMV-Foxm1* or *CMV-Foxf1* plasmids. These data indicate that nanoparticle delivery of FOXM1 or FOXF1 is needed to stimulate lung regeneration after hyperoxic injury.

Rodent models of BPD often use excessive periods of hyperoxia. The hyperoxic treatment in this study used a more relevant 7-day, 75% O_2 exposure that still induced significant alveolar simplification and impaired lung function, as shown previously (48). Although this mouse model causes lung structural and functional impairments similar to those in human BPD, this model does not take into account the effects of mechanical ventilation or recapitulate the effects of being born premature. Nonetheless, this represents a highly reproducible and easily accessible model of lung simplification that can be used to generate data about the efficacy of novel therapeutic options.

Cell proliferation has previously been shown to be compromised in BPD lungs as well as in animals exposed to neonatal hyperoxia (5, 47). Hyperoxia inhibited cell cycle progression in endothelial cell lines and primary lung endothelial cells *in vitro* (5, 47). In the present study, we found that nanoparticle delivery of FOXM1 or FOXF1 inhibited the expression of FOXO1 in hyperoxia-treated lungs. Because FOXO1 reduces cell cycle progression during organ morphogenesis, repair, and regeneration (46), inhibition of FOXO1 can contribute to increased endothelial proliferation in lungs treated with nanoparticle–DNA complexes. Furthermore, FOXM1 and FOXF1 delivered by the nanoparticles can bind to the evolutionarily conserved FOX DNA-binding motifs vacated by the FOXO1 protein, alleviating FOXO1-mediated transcriptional repression of cell cycle regulatory genes. Consistent with this hypothesis, FOXM1 and FOXO1 have been shown to compete for the same DNA-binding sites, differentially regulating gene expression in developing cardiomyocytes (50).

Changes in elastin organization have previously been reported for BPD and other respiratory diseases and have significant consequences for lung function (5, 8, 12). Elastin organization is important developmentally for the formation of secondary septa, which increase alveolar gas exchange area and provide a niche for development of the complex network of pulmonary capillaries. Consistent with published studies (5, 12), we found that hyperoxia exposure leads to disorganization of elastin fibers in alveolar septa, findings supported by changes in the pressure–volume loop area and lung compliance. Elastin fiber organization was improved after nanoparticle delivery of FOXM1 and FOXF1. Alveolar myofibroblasts are primarily responsible for elastin production and deposition of elastin fibers into the alveolar septa (12), and they were also targeted by this gene delivery method. Increased elastin deposition can be a direct effect of FOXM1 and FOXF1 on elastin expression or homeostasis in pulmonary myofibroblasts.

In summary, we tested a novel formulation of nanoparticles efficiently delivering nonintegrating expression plasmids into microvascular endothelial cells and myofibroblasts in the neonatal lung. Delivery of FOXM1 or FOXF1, both

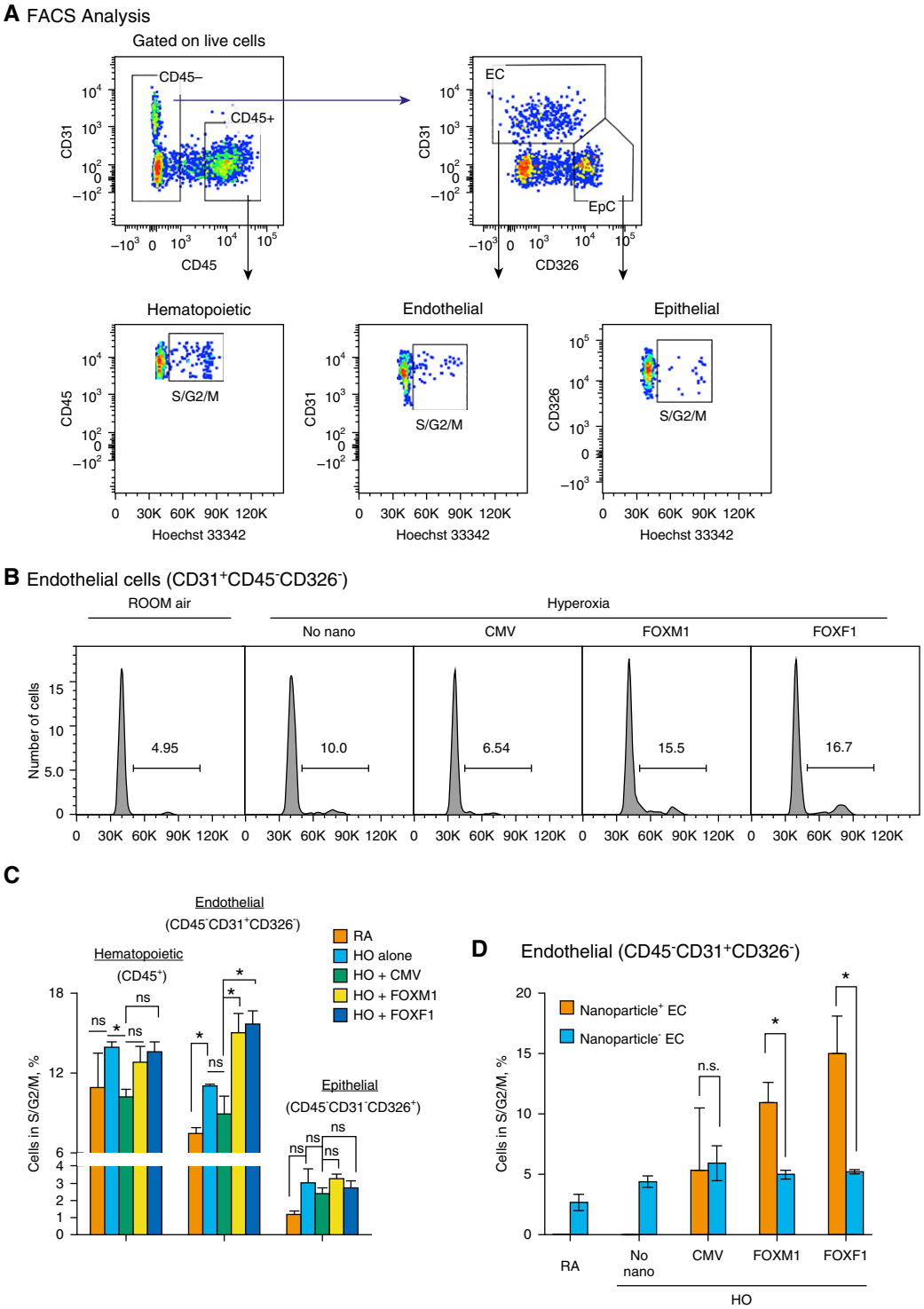

Figure 7. Nanoparticle delivery of FOXM1 (forkhead box M1) or FOXF1 (forkhead box F1) increases endothelial cell proliferation during the recovery period after neonatal hyperoxia (HO). (*A*) Fluorescence-activated cell sorter (FACS) gating strategy to identify hematopoietic ($CD45^+CD31^-$), epithelial (EpC; $CD326^+CD45^-CD31^-$), and endothelial cells (EC; $CD31^+CD45^-CD326^-$) in mouse lung tissue. Mice were exposed to HO or room air (RA) from Postnatal Day 1 (P1) to P7, followed by RA exposure. FACS analysis of enzymatically digested lung tissue was performed 2 days after injury at P9. Dot plots show FACS analysis of cells obtained from HO-treated lungs. Hoechst 33342 dye was used to identify cells undergoing S, G_2, and M phases of the cell cycle. (*B* and *C*) Histograms in *B* show the percentage of EC in S, G_2, and M phases of the cell cycle after nanoparticle delivery of FOXM1 or FOXF1 compared with cytomegalovirus (CMV)-empty control. Data were quantitated in *C* and compared between different pulmonary cell types ($n = 3$–4 mice per group). Nanoparticle delivery of FOXM1 or FOXF1 increases the percentage of proliferating EC in HO-treated lungs. (*D*) Comparison of EC with and without nanoparticles. Cell proliferation is higher in EC containing nanoparticles with FOXM1 or FOXF1 ($Nanoparticle^+$ EC) than in EC without nanoparticles ($Nanoparticle^-$ EC) ($n = 3$–4 mice per group). Error bars are mean ± SE. $^*P < 0.05$. n.s. = not significant.

downstream targets of VEGF, did not protect endothelial cells from apoptosis caused by hyperoxia, but it increased endothelial proliferation and lung angiogenesis after the injury. Our results suggest that nanoparticle delivery of proangiogenic transcription factors can be beneficial to improve lung structure and function in a subset of patients with BPD with pulmonary vascular disease. ■

Author disclosures are available with the text of this article at www.atsjournals.org.

Acknowledgment: The authors gratefully thank Dr. Kofron for help with confocal microscopy.

References

1. Ohtani S, Iwamaru A, Deng W, Ueda K, Wu G, Jayachandran G, *et al*. Tumor suppressor 101F6 and ascorbate synergistically and selectively inhibit non–small cell lung cancer growth by caspase-independent apoptosis and autophagy. *Cancer Res* 2007;67: 6293–6303.
2. Horiguchi M, Kojima H, Sakai H, Kubo H, Yamashita C. Pulmonary administration of integrin-nanoparticles regenerates collapsed alveoli. *J Control Release* 2014;187:167–174.
3. Naderi N, Karponis D, Mosahebi A, Seifalian AM. Nanoparticles in wound healing; from hope to promise, from promise to routine. *Front Biosci* 2018;23:1038–1059.
4. Jiang X, Malkovskiy AV, Tian W, Sung YK, Sun W, Hsu JL, *et al*. Promotion of airway anastomotic microvascular regeneration and alleviation of airway ischemia by deferoxamine nanoparticles. *Biomaterials* 2014;35:803–813.
5. Abman SH. Impaired vascular endothelial growth factor signaling in the pathogenesis of neonatal pulmonary vascular disease. *Adv Exp Med Biol* 2010;661:323–335.
6. Northway WH Jr, Rosan RC, Porter DY. Pulmonary disease following respirator therapy of hyaline-membrane disease: bronchopulmonary dysplasia. *N Engl J Med* 1967;276:357–368.
7. Stenmark KR, Abman SH. Lung vascular development: implications for the pathogenesis of bronchopulmonary dysplasia. *Annu Rev Physiol* 2005;67:623–661.
8. Thébaud B, Abman SH. Bronchopulmonary dysplasia: where have all the vessels gone? Roles of angiogenic growth factors in chronic lung disease. *Am J Respir Crit Care Med* 2007;175:978–985.
9. Bhatt AJ, Pryhuber GS, Huyck H, Watkins RH, Metlay LA, Maniscalco WM. Disrupted pulmonary vasculature and decreased vascular endothelial growth factor, Flt-1, and TIE-2 in human infants dying with bronchopulmonary dysplasia. *Am J Respir Crit Care Med* 2001;164: 1971–1980.
10. Thébaud B, Ladha F, Michelakis ED, Sawicka M, Thurston G, Eaton F, *et al*. Vascular endothelial growth factor gene therapy increases survival, promotes lung angiogenesis, and prevents alveolar damage in hyperoxia-induced lung injury: evidence that angiogenesis participates in alveolarization. *Circulation* 2005;112:2477–2486.
11. Kunig AM, Balasubramaniam V, Markham NE, Morgan D, Montgomery G, Grover TR, *et al*. Recombinant human VEGF treatment enhances alveolarization after hyperoxic lung injury in neonatal rats. *Am J Physiol Lung Cell Mol Physiol* 2005;289:L529–L535.
12. Whitsett JA, Kalin TV, Xu Y, Kalinichenko VV. Building and regenerating the lung cell by cell. *Physiol Rev* 2019;99:513–554.
13. Bolte C, Whitsett JA, Kalin TV, Kalinichenko VV. Transcription factors regulating embryonic development of pulmonary vasculature. *Adv Anat Embryol Cell Biol* 2018;228:1–20.
14. Hoffmann AD, Yang XH, Burnicka-Turek O, Bosman JD, Ren X, Steimle JD, *et al*. *Foxf* genes integrate *Tbx5* and Hedgehog pathways in the second heart field for cardiac septation. *PLoS Genet* 2014;10:e1004604.
15. Balli D, Ren X, Chou FS, Cross E, Zhang Y, Kalinichenko VV, *et al*. Foxm1 transcription factor is required for macrophage migration during lung inflammation and tumor formation. *Oncogene* 2012;31:3875–3888.
16. Ramakrishna S, Kim IM, Petrovic V, Malin D, Wang IC, Kalin TV, *et al*. Myocardium defects and ventricular hypoplasia in mice homozygous null for the forkhead box M1 transcription factor. *Dev Dyn* 2007;236: 1000–1013.
17. Ustiyan V, Wert SE, Ikegami M, Wang IC, Kalin TV, Whitsett JA, *et al*. Foxm1 transcription factor is critical for proliferation and differentiation of Clara cells during development of conducting airways. *Dev Biol* 2012;370:198–212.
18. Cai Y, Bolte C, Le T, Goda C, Xu Y, Kalin TV, *et al*. FOXF1 maintains endothelial barrier function and prevents edema after lung injury. *Sci Signal* 2016;9:ra40.
19. Bolte C, Flood HM, Ren X, Jagannathan S, Barski A, Kalin TV, *et al*. FOXF1 transcription factor promotes lung regeneration after partial pneumonectomy. *Sci Rep* 2017;7:10690.
20. Kim IM, Ramakrishna S, Gusarova GA, Yoder HM, Costa RH, Kalinichenko VV. The forkhead box m1 transcription factor is essential for embryonic development of pulmonary vasculature. *J Biol Chem* 2005;280:22278–22286.
21. Kalinichenko VV, Zhou Y, Shin B, Stolz DB, Watkins SC, Whitsett JA, *et al*. Wild-type levels of the mouse Forkhead Box f1 gene are essential for lung repair. *Am J Physiol Lung Cell Mol Physiol* 2002; 282:L1253–L1265.
22. Ren X, Ustiyan V, Pradhan A, Cai Y, Havrilak JA, Bolte CS, *et al*. FOXF1 transcription factor is required for formation of embryonic vasculature by regulating VEGF signaling in endothelial cells. *Circ Res* 2014;115:709–720.
23. Dharmadhikari AV, Szafranski P, Kalinichenko VV, Stankiewicz P. Genomic and epigenetic complexity of the FOXF1 locus in 16q24.1: implications for development and disease. *Curr Genomics* 2015;16: 107–116.
24. Pradhan A, Dunn A, Ustiyan V, Bolte C, Wang G, Whitsett JA, *et al*. The S52F FOXF1 mutation inhibits STAT3 signaling and causes alveolar capillary dysplasia. *Am J Respir Crit Care Med* 2019;200: 1045–1056.
25. Bishop NB, Stankiewicz P, Steinhorn RH. Alveolar capillary dysplasia. *Am J Respir Crit Care Med* 2011;184:172–179.
26. Dunn AW, Kalinichenko VV, Shi D. Highly efficient *in vivo* targeting of the pulmonary endothelium using novel modifications of polyethylenimine: an importance of charge. *Adv Healthc Mater* 2018; 7:e1800876.
27. Xia H, Ren X, Bolte CS, Ustiyan V, Zhang Y, Shah TA, *et al*. Foxm1 regulates resolution of hyperoxic lung injury in newborns. *Am J Respir Cell Mol Biol* 2015;52:611–621.
28. Hoggatt AM, Kim JR, Ustiyan V, Ren X, Kalin TV, Kalinichenko VV, *et al*. The transcription factor Foxf1 binds to serum response factor and myocardin to regulate gene transcription in visceral smooth muscle cells. *J Biol Chem* 2013;288:28477–28487.
29. Milewski D, Pradhan A, Wang X, Cai Y, Le T, Turpin B, *et al*. FoxF1 and FoxF2 transcription factors synergistically promote rhabdomyosarcoma carcinogenesis by repressing transcription of $p21^{Cip1}$ CDK inhibitor. *Oncogene* 2017;36:850–862.
30. Milewski D, Balli D, Ustiyan V, Le T, Dienemann H, Warth A, *et al*. FOXM1 activates AGR2 and causes progression of lung adenomas into invasive mucinous adenocarcinomas. *PLoS Genet* 2017;13: e1007097.
31. Black M, Milewski D, Le T, Ren X, Xu Y, Kalinichenko VV, *et al*. FOXF1 inhibits pulmonary fibrosis by preventing CDH2-CDH11 cadherin switch in myofibroblasts. *Cell Rep* 2018;23: 442–458.
32. Ustiyan V, Bolte C, Zhang Y, Han L, Xu Y, Yutzey KE, *et al*. FOXF1 transcription factor promotes lung morphogenesis by inducing cellular proliferation in fetal lung mesenchyme. *Dev Biol* 2018;443: 50–63.
33. Kalinichenko VV, Gusarova GA, Shin B, Costa RH. The forkhead box F1 transcription factor is expressed in brain and head mesenchyme during mouse embryonic development. *Gene Expr Patterns* 2003;3: 153–158.
34. Kim IM, Zhou Y, Ramakrishna S, Hughes DE, Solway J, Costa RH, *et al*. Functional characterization of evolutionarily conserved DNA regions in forkhead box f1 gene locus. *J Biol Chem* 2005;280:37908–37916.

35. Wang X, Bhattacharyya D, Dennewitz MB, Kalinichenko VV, Zhou Y, Lepe R, *et al*. Rapid hepatocyte nuclear translocation of the forkhead box M1B (FoxM1B) transcription factor caused a transient increase in size of regenerating transgenic hepatocytes. *Gene Expr* 2003;11: 149–162.
36. Ren X, Ustiyan V, Guo M, Wang G, Bolte C, Zhang Y, *et al*. Postnatal alveologenesis depends on FOXF1 signaling in c-KIT$^+$ endothelial progenitor cells. *Am J Respir Crit Care Med* 2019;200: 1164–1176.
37. Wang IC, Meliton L, Ren X, Zhang Y, Balli D, Snyder J, *et al*. Deletion of forkhead box M1 transcription factor from respiratory epithelial cells inhibits pulmonary tumorigenesis. *PLoS One* 2009; 4:e6609.
38. Wang IC, Snyder J, Zhang Y, Lander J, Nakafuku Y, Lin J, *et al*. Foxm1 mediates cross talk between Kras/mitogen-activated protein kinase and canonical Wnt pathways during development of respiratory epithelium. *Mol Cell Biol* 2012;32:3838–3850.
39. Bolte C, Zhang Y, Wang IC, Kalin TV, Molkentin JD, Kalinichenko VV. Expression of Foxm1 transcription factor in cardiomyocytes is required for myocardial development. *PLoS One* 2011;6: e22217.
40. Cheng XH, Black M, Ustiyan V, Le T, Fulford L, Sridharan A, *et al*. SPDEF inhibits prostate carcinogenesis by disrupting a positive feedback loop in regulation of the Foxm1 oncogene. *PLoS Genet* 2014;10:e1004656.
41. Pradhan A, Ustiyan V, Zhang Y, Kalin TV, Kalinichenko VV. Forkhead transcription factor FoxF1 interacts with Fanconi anemia protein complexes to promote DNA damage response. *Oncotarget* 2016;7: 1912–1926.
42. Bolte C, Ren X, Tomley T, Ustiyan V, Pradhan A, Hoggatt A, *et al*. Forkhead box F2 regulation of platelet-derived growth factor and myocardin/serum response factor signaling is essential for intestinal development. *J Biol Chem* 2015;290:7563–7575.
43. Sun L, Ren X, Wang IC, Pradhan A, Zhang Y, Flood HM, *et al*. The FOXM1 inhibitor RCM-1 suppresses goblet cell metaplasia and prevents IL-13 and STAT6 signaling in allergen-exposed mice. *Sci Signal* 2017;10:eaai8583.
44. Ren X, Zhang Y, Snyder J, Cross ER, Shah TA, Kalin TV, *et al*. Forkhead box M1 transcription factor is required for macrophage recruitment during liver repair. *Mol Cell Biol* 2010;30:5381–5393.
45. Kalin TV, Meliton L, Meliton AY, Zhu X, Whitsett JA, Kalinichenko VV. Pulmonary mastocytosis and enhanced lung inflammation in mice heterozygous null for the Foxf1 gene. *Am J Respir Cell Mol Biol* 2008; 39:390–399.
46. Wilhelm K, Happel K, Eelen G, Schoors S, Oellerich MF, Lim R, *et al*. FOXO1 couples metabolic activity and growth state in the vascular endothelium. *Nature* 2016;529:216–220.
47. Shivanna B, Maity S, Zhang S, Patel A, Jiang W, Wang L, *et al*. Gene expression profiling identifies cell proliferation and inflammation as the predominant pathways regulated by aryl hydrocarbon receptor in primary human fetal lung cells exposed to hyperoxia. *Toxicol Sci* 2016;152:155–168.
48. Willis GR, Fernandez-Gonzalez A, Anastas J, Vitali SH, Liu X, Ericsson M, *et al*. Mesenchymal stromal cell exosomes ameliorate experimental bronchopulmonary dysplasia and restore lung function through macrophage immunomodulation. *Am J Respir Crit Care Med* 2018;197:104–116.
49. Kunig AM, Balasubramaniam V, Markham NE, Seedorf G, Gien J, Abman SH. Recombinant human VEGF treatment transiently increases lung edema but enhances lung structure after neonatal hyperoxia. *Am J Physiol Lung Cell Mol Physiol* 2006;291: L1068–L1078.
50. Sengupta A, Kalinichenko VV, Yutzey KE. FoxO1 and FoxM1 transcription factors have antagonistic functions in neonatal cardiomyocyte cell-cycle withdrawal and IGF1 gene regulation. *Circ Res* 2013;112:267–277.